

Thermo-mechanical Systems with Several Heat Reservoirs: Maximum Power Processes

S.A. Amelkin[†], B. Andresen[‡], J.M. Burzler[★],
K.H. Hoffmann[★], and A.M. Tsirlin[†]

[†]Program Systems Institute,
RU-152140 Pereslavl-Zalessky, Russia

[‡]Ørsted Laboratory, University of Copenhagen,
Universitetsparken 5, DK-2100 Copenhagen Ø, Denmark

[★] Institute of Physics, Technical University of Chemnitz,
D-09107 Chemnitz, Germany

July 22, 2004

Abstract

While endoreversible heat-to-power conversion systems operating between two heat reservoirs have been intensely studied, systems with several reservoirs have attracted little attention. Here we analyse the maximum power processes of such systems with stationary temperature reservoirs. We find that independent of the number of reservoirs the working fluid uses only two isotherms and two infinitely fast isentropes/adiabats. One surprising result is that there may be reservoirs which are never used. This feature is explained for a simple system with three heat reservoirs.

1 Introduction

Finite-time thermodynamics provides tools for deriving fundamental bounds and optimal parameters for the performance of thermo-mechanical systems operating at non-zero flows or at finite process durations. Within this theory thermo-mechanical systems are often modelled as endoreversible systems [1–3] consisting of equilibrium subsystems which are, in general, not in equilibrium with one another but are interacting via irreversible heat transfer processes. The field of finite-time thermodynamics has experienced intense research activity during the last twenty years, at least initially with an emphasis on thermo-mechanical systems operating between two heat reservoirs (see [3, 4] for reviews).

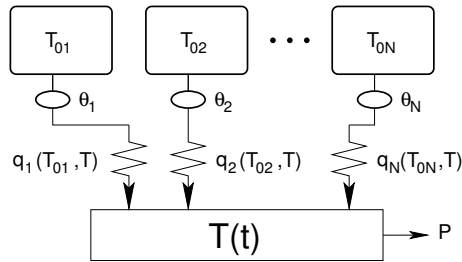


Figure 1: Model of an endoreversible heat engine connected to several heat reservoirs.

Several authors have also studied staged and combined systems (see [5–14] for example), yet endoreversible systems with more than two fixed heat reservoirs have been neglected in the literature so far despite the fact that such arrangements are common for many real-world applications such as industrial heat recovery systems and solar energy installations.

The present paper tries to fill this gap and investigates endoreversible heat engines with an arbitrary number of heat reservoirs using the average power output as a criterion of thermodynamic merit. Methods of averaged nonlinear programming [15, 16], which are already well established for the optimisation of thermo-mechanical systems with two heat reservoirs [17–19], are applied to determine the maximum possible average power output and optimal contact functions between the heat reservoirs and a power converting subsystem. The analysis covers both cyclic and one-shot processes. The temperatures of the heat reservoirs are assumed constant.

2 System description

In this section we introduce the system we analyse and formalize the problem of maximum power operation. The system at issue is depicted in Fig.1 and consists of a power converting subsystem with a working fluid at one unique temperature $T(t)$ at each moment of time and N heat reservoirs at temperatures T_{0i} with $i \in [1, N]$. The heat transfer law for each reservoir has the form

$$\tilde{q}_i(T_{0i}, T, \theta_i) = \theta_i q_i(T_{0i}, T). \quad (1)$$

The contact functions θ_i describe the extent of the contact between reservoir and engine. They are equal to one, when the working fluid is fully connected with the i -th reservoir and are equal to zero when there is no contact. Thus $0 \leq \theta_i \leq 1$.

We further assume that

- the working fluid in the power converting subsystem is in internal equilibrium and is thus characterised by one unique value of its temperature

$T(t)$ at each moment of time;

- the processes in the reservoirs and in the power converting subsystem are reversible (i.e. the endoreversibility hypothesis [6]);
- all irreversibilities are associated with the interactions between the working fluid and the heat reservoirs, i.e. other possible irreversibilities in heat engines for instance due to friction are not included;
- the transfer functions $q_i(T_{0i}, T)$ satisfy common requirements for monotonicity in T_{0i} and T , i.e. heat flows from high to low temperatures: $q_i(T_{0i}, T) > 0$ if $T_{0i} > T$, $q_i(T_{0i}, T) < 0$ if $T_{0i} < T$, and $q_i(T_{0i}, T) = 0$ if $T_{0i} = T$;
- durations of isentropic/adiabatic processes vanish as we neglect friction and inertia.

In the following we investigate a system where the temperatures T_{0i} of all heat reservoirs are constant in time and the working fluid is subject to a given averaged rate of change in internal energy \bar{u} and entropy $\bar{\sigma}$ during a process of fixed duration τ .

3 Power optimized processes

The aim of this section is to characterize the maximum averaged power operation of the above introduced system. We take the fluid temperature $T(t)$ and the contact functions $\theta_i(T_{0i}, T)$ as the $N + 1$ controls to optimise the average power output of the system. To formalize the problem we introduce the energy and entropy balances for the working fluid.

Due to the first law the average power output \bar{P} and the averaged sum of the heat flows

$$\bar{q} = \frac{1}{\tau} \int_0^\tau \sum_{i=1}^N \theta_i q_i(T_{0i}, T) dt \quad (2)$$

differ only by the averaged rate of change in internal energy

$$\bar{P} = \bar{q} - \bar{u} . \quad (3)$$

Thus the maximization of the average power output is equivalent to the maximisation of averaged sum of heat flows.

Maximum power output processes are thus determined by

$$\bar{q} = \frac{1}{\tau} \int_0^\tau \sum_{i=1}^N \theta_i q_i(T_{0i}, T) dt \rightarrow \max_{T, \theta} \quad (4)$$

subject to the restriction given by the entropy balance

$$\frac{1}{\tau} \int_0^\tau \frac{1}{T} \sum_{i=1}^N \theta_i q_i(T_{0i}, T) dt = \bar{\sigma} . \quad (5)$$

The values of $\bar{\sigma}$ and \bar{u} are zero for cyclic processes and the process time τ is the cycle time.

The controls of the process, which are the temperature $T(t)$ of the working fluid and the elements of the vector $\boldsymbol{\theta}(t) = (\theta_1, \theta_2, \dots, \theta_N)$ of the contact functions, satisfy the following properties:

$$\theta_i(t) \in [0, 1] \quad \text{and} \quad T(t) > 0. \quad (6)$$

Solving equations (4–6) would usually require the use of optimal control theory. However, the special structure of equations (4–6) define a problem of averaged nonlinear programming [15, 16], as the objective function (the power) as well as the the constraint (the entropy change) are quantities averaged over the process time. A special theory can be used to solve such problems [20] which we recapitulate below to the extent necessary.

3.1 Optimal contact functions

Equations (4–6) define a problem of averaged nonlinear programming. The optimality condition for this problem has the form

$$\mathcal{L} = \sum_{i=1}^N \theta_i q_i(T_{0i}, T) \left[1 - \frac{\lambda}{T} \right] \rightarrow \max_{T, \boldsymbol{\theta}}. \quad (7)$$

Let us first consider the variation of \mathcal{L} with respect to each of the contact functions $\theta_i(T_{0i}, T)$. The Lagrange function \mathcal{L} is linearly dependent on each θ_i , so the maximum can only be situated at the boundary of the admissible range of θ_i . The boundary values $\{0, 1\}$ of θ_i , through the Pontryagin maximum principle, determine a rule for the contact functions:

$$\theta_i(T_{0i}, T) = \begin{cases} 1, & \text{if } [1 - \lambda/T]q_i(T_{0i}, T) > 0 \\ 0, & \text{if } [1 - \lambda/T]q_i(T_{0i}, T) < 0 \end{cases} \quad i \in [1, N]. \quad (8)$$

Let us take a closer look at this rule, eq. (8). If T is less than λ then $q_i(T_{0i}, T)$ needs to be negative. This means that the working fluid is in contact with reservoirs serving as heat sinks and fulfilling the condition $T_{0i} < T$. In the opposite case, when T is greater than λ , the heat flow $q_i(T_{0i}, T)$ must be positive implying the condition $T_{0i} > T$. The working fluid connects to reservoirs acting as heat sources. In effect the rule (8) divides the set of N heat reservoirs into two subsets of *hot* and *cold* reservoirs, respectively. Depending on the value of T (greater or less than λ) the working fluid in the power converting subsystem is either connected to reservoirs of the hot or cold set.

3.2 Constructing heating and cooling functions

To be more explicit about the heat flows resulting from the above rule, the heat transfer function for each reservoir can be split into heat input and output

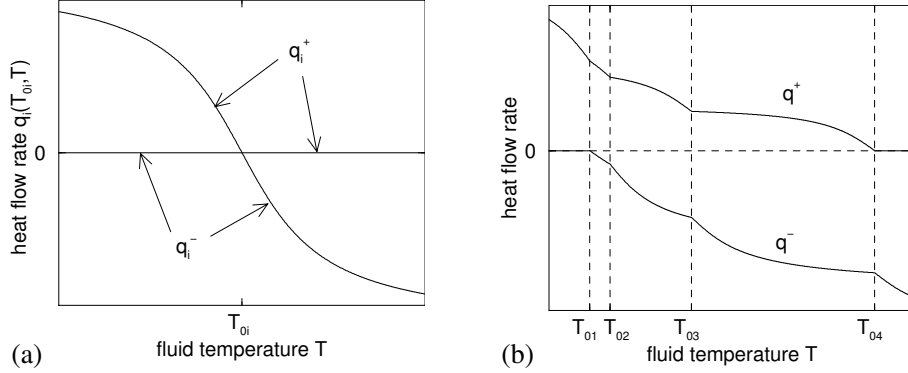


Figure 2: An example of four heat reservoirs at different temperatures $T_{01} < T_{02} < T_{03} < T_{04}$ which are connected to the working fluid via non-linear heat transfer. The heat input $q_i^+(T_{0i}, T)$, and output $q_i^-(T_{0i}, T)$ functions for each reservoir (left) are combined to total heat input $q^+(\mathbf{T}_0, T)$ and output $q^-(\mathbf{T}_0, T)$ functions (right).

functions:

$$q_i^+(T_{0i}, T) = \begin{cases} q_i(T_{0i}, T), & \text{if } T_{0i} \geq T, \\ 0, & \text{if } T_{0i} < T, \end{cases} \quad i \in [1, N]; \quad (9)$$

$$q_i^-(T_{0i}, T) = \begin{cases} 0, & \text{if } T_{0i} > T, \\ q_i(T_{0i}, T), & \text{if } T_{0i} \leq T, \end{cases} \quad i \in [1, N]. \quad (10)$$

The total rate of heat input $q^+(\mathbf{T}_0, T)$ or output $q^-(\mathbf{T}_0, T)$ to and from the working fluid is then simply the sum of all contributions $q_i^+(\mathbf{T}_0, T)$ and $q_i^-(\mathbf{T}_0, T)$,

$$q^+(\mathbf{T}_0, T) = \sum_{i=1}^N q_i^+(T_{0i}, T) \quad (11)$$

$$q^-(\mathbf{T}_0, T) = \sum_{i=1}^N q_i^-(T_{0i}, T). \quad (12)$$

The abbreviation $\mathbf{T}_0 = (T_{01}, T_{02}, \dots, T_{0N})$ denotes the vector of reservoir temperatures.

Figure 2 illustrates the above construction of heating and cooling functions for an example of four heat reservoirs at different temperatures and non-linear heat transfer. Definitions (9–12) and rule (8) can be used to introduce a function of total heat exchange,

$$q_\Sigma(\mathbf{T}_0, T) = \sum_{i=1}^N \theta_i q_i(T_{0i}, T) = \begin{cases} q^+(\mathbf{T}_0, T), & \text{if } T > \lambda \\ q^-(\mathbf{T}_0, T), & \text{if } T < \lambda \end{cases} \quad (13)$$

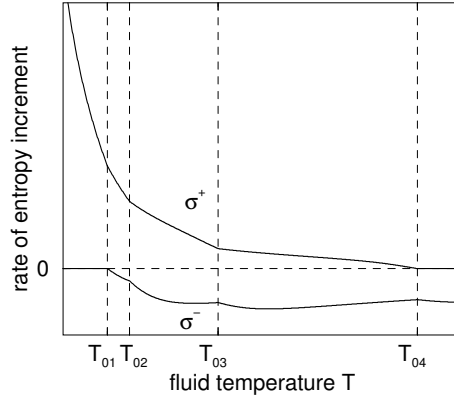


Figure 3: Entropy change rates $\sigma^-(\mathbf{T}_0, T)$ and $\sigma^+(\mathbf{T}_0, T)$ for heat inflow and outflow, respectively, versus the temperature T of the working fluid.

which shows a discontinuity at $T = \lambda$ where there is a jump from q^- to q^+ .

The heat exchange causes an entropy change of the working fluid in the reversible compartment. The entropy flows to the working fluid are easily obtained by dividing the corresponding heat exchange rates by the current temperature of the working fluid. In particular, the total rate of entropy increase of the working fluid is

$$\sigma_{\Sigma}(\mathbf{T}_0, T) = \frac{q_{\Sigma}(\mathbf{T}_0, T)}{T} = \begin{cases} \sigma^+(\mathbf{T}_0, T), & \text{if } T > \lambda \\ \sigma^-(\mathbf{T}_0, T), & \text{if } T < \lambda \end{cases} \quad (14)$$

where

$$\sigma^+(\mathbf{T}_0, T) = \frac{q^+(\mathbf{T}_0, T)}{T} \quad \text{and} \quad \sigma^-(\mathbf{T}_0, T) = \frac{q^-(\mathbf{T}_0, T)}{T}. \quad (15)$$

It is easily seen that $q_{\Sigma}(\mathbf{T}_0, T)$ is the integrand of the objective functional (4) and $\sigma_{\Sigma}(\mathbf{T}_0, T)$ is the integrand of the restriction (5) of the optimisation problem. Since the functions q^+ , q^- , σ^+ and σ^- are independent of λ , and q^+ , q^- are additionally monotonic in T , the relations $\sigma^+(q^+)$ and $\sigma^-(q^-)$ are well defined and cover distinct ranges with the exception of the origin as the only common point. Therefore we can combine the two branches, $\sigma^+(q^+)$ and $\sigma^-(q^-)$, to one relation $\sigma(q)$ as illustrated in Figure 4.

3.3 Optimal temperatures of the working fluid

The theory of averaged programming [15, 16] states that the solution for the optimal controls are piecewise constant functions taking values from a set of no more than $l + 1$ *base points* where l is the number of averaged constraints

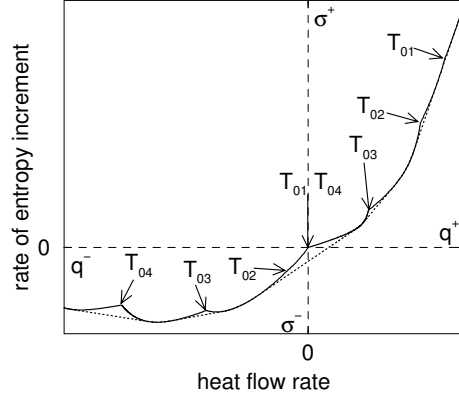


Figure 4: The relation $\sigma(q)$ between the rates of entropy increment σ and heat flow rate q consists of two branches $\sigma^+(q^+)$ and $\sigma^-(q^-)$ which have the origin of the graph as one common point. The lower border of the convex hull of $\sigma(q)$ is drawn as a dotted line.

of the problem. There is only one constraint, the entropy balance of eq. (5) in our study, and consequently there are no more than two base points for the temperature T . These base points are located at points where the function $\sigma(q)$ coincides with the lower border of its convex hull. Figure 4 illustrates that points corresponding to a temperature T equal to a reservoir temperature T_{0i} are not on the lower border of the convex hull since the contacts to heat reservoirs are switching at reservoir temperatures. This results in a sudden decrease of the slope of $\sigma(q)$ at the kinks in the curve of $\sigma(q)$.

Let us denote the two base points of the fluid temperature as T_1 and T_2 . If the value of $\bar{\sigma}$ is located on the lower border convex hull of $\sigma(q)$, the two base points T_1 and T_2 are identical and there is actually only one base point. Without loss of generality we now proceed with two (not necessarily distinct) base points. The Lagrange function (7) reaches its maximum at the base points so that the optimality condition $\partial\mathcal{L}/\partial T = 0$, which can be written as

$$\lambda = \frac{\partial q_\Sigma}{\partial T} T \left(\frac{\partial q_\Sigma}{\partial T} - \frac{q_\Sigma(\mathbf{T}_0, T)}{T} \right)^{-1}, \quad (16)$$

is fulfilled at $T = T_1$ and $T = T_2$.

Another optimality condition is determined from the equality of the Lagrangian at the base values, $\mathcal{L}(\lambda, T_1) = \mathcal{L}(\lambda, T_2)$, expressed as

$$q_\Sigma(\mathbf{T}_0, T_1) \left[1 - \frac{\lambda}{T_1} \right] = q_\Sigma(\mathbf{T}_0, T_2) \left[1 - \frac{\lambda}{T_2} \right]. \quad (17)$$

Restriction (5) on the average rate of entropy change of the working fluid gives an equation which can be used to obtain the parts γ_1 and γ_2 of the process time

τ spent at the corresponding base points T_1 and T_2

$$\gamma_1 \frac{q_\Sigma(\mathbf{T}_0, T_1)}{T_1} + \gamma_2 \frac{q_\Sigma(\mathbf{T}_0, T_2)}{T_2} = \bar{\sigma}, \quad (18)$$

with

$$\gamma_1 + \gamma_2 = 1, \gamma_1 \geq 0, \gamma_2 \geq 0. \quad (19)$$

Equations (16–19) determine the values of λ , T_1 , T_2 , γ_1 , and γ_2 for given laws of heat conduction $q_i(T_{0i}, T)$, reservoir temperatures T_{0i} and average rates of change for the entropy $\bar{\sigma}$ and internal energy \bar{u} of the working fluid. These equations are used to analytically or numerically calculate optimal solutions. Note that the optimal solutions for the controls are not unique if there is more than one base value, because the functionals (4) and (5) are independent of the order in which the controls take their base values.

3.4 Optimal solution for cyclic systems

A cyclic operating regime is characterised by vanishing average rates of entropy $\bar{\sigma}$ and internal energy \bar{u} . These conditions allows us to simplify equation (18) to

$$\frac{\gamma_2}{\gamma_1} = -\frac{T_2 q_\Sigma(\mathbf{T}_0, T_1)}{T_1 q_\Sigma(\mathbf{T}_0, T_2)}. \quad (20)$$

The ratio $q_\Sigma(\mathbf{T}_0, T_1)/q_\Sigma(\mathbf{T}_0, T_2)$ in the above expression can be eliminated using equation (17). The resulting expression is further simplified with condition (19) to

$$\lambda = \gamma_1 T_2 + \gamma_2 T_1. \quad (21)$$

Let us discuss the meaning of this result. It is immediately clear from condition (19) that the value of λ is between the values of the base points T_1 and T_2 . The cases where one or two of the base points are equal to λ is of little interest here since this would correspond to zero heat input or output as can be seen from equations (16) and (17). We therefore can assume that one base value, now denoted T^+ , is larger than λ and the other one, now denoted T^- , is smaller than λ .

The rule (8) for the contact function implies that the base value T^+ is associated with heat input from reservoirs with temperatures larger than T^+ while the value T^- is associated with heat output to reservoirs at temperatures smaller than T^- . All reservoirs with temperatures in the range between T^- and T^+ are therefore never connected during a cycle; these reservoirs are called *unused* reservoirs.

Let us take a closer look at the example presented in figs. 2 to 4 to explain how one can distinguish between used and unused reservoirs and how optimal solutions are obtained. Figure 5 shows a detail of the $\sigma(q)$ relation depicted in fig. 4. The two base points T^- and T^+ of the optimal solution are located at the lower left and upper right corner of the graph in fig. 5. The heat flows at

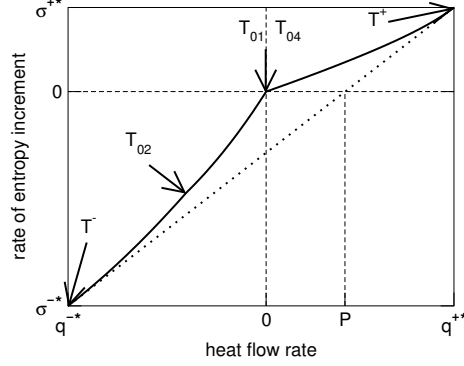


Figure 5: The optimal solution for $\bar{\sigma} = 0$ is the average of the two base points T^- and T^+ corresponding to heat and entropy outflow (q^{-*}, σ^{-*}) and inflow (q^{+*}, σ^{+*}) , respectively, and leading to an average power output \bar{P} .

these points are

$$q^{+*} = q^+(\mathbf{T}_0, T^+) = q_\Sigma(\mathbf{T}_0, T^+) \quad (22)$$

$$q^{-*} = q^-(\mathbf{T}_0, T^-) = q_\Sigma(\mathbf{T}_0, T^-) . \quad (23)$$

The base points are easily found geometrically by starting at the origin where the restriction $\sigma = \bar{\sigma} = 0$ is fulfilled and travelling in the two opposite directions on the $\sigma(q)$ curve until the lower border of the convex hull of $\sigma(q)$ is touched. All points on the negative branch of the graph from the origin to the base point (q^{-*}, σ^{-*}) correspond to increasing temperatures from T_{01} to T^- , all points on the positive branch of the graph from the origin to the base point (q^{+*}, σ^{+*}) correspond to decreasing temperatures from T_{04} to T^+ . This means that reservoirs whose temperatures are between T^- and T^+ , i.e. outside the range (q^{-*}, σ^{-*}) and (q^{+*}, σ^{+*}) on the $\sigma(q)$ curve, are unused reservoirs.

In our example, the working fluid alternately operates at the temperature T^- where it rejects heat to the two coldest reservoirs (T_{02} and T_{01}) and at the temperature T^+ where it receives heat from the hottest reservoir (T_{04}). The working fluid however never connects to the reservoir with the intermediate temperature T_{03} .

The parts of time γ^+ and γ^- spent at either base point can be determined analytically. Substitute the two occurrences of λ into equation (17) by the two instances of equation (16). By considering the notation for the two base points T^+ and T^- one obtains

$$\left(\frac{T^- q^{+*}}{T^+ q^{-*}} \right)^2 = \frac{(\partial q^+ / \partial T)|_{T^+}}{(\partial q^- / \partial T)|_{T^-}} . \quad (24)$$

Then substitute the left side of the above equation by equation (20) and take

the squareroot to get an expression for the ratio of the parts

$$\frac{\gamma^-}{\gamma^+} = \sqrt{\frac{(\partial q^+/\partial T)|_{T^+}}{(\partial q^-/\partial T)|_{T^-}}}. \quad (25)$$

The values for each part are readily derived using equation (18), $\gamma^+ + \gamma^- = 1$:

$$\gamma^+ = \frac{\sqrt{-(\partial q^-/\partial T)|_{T^-}}}{\sqrt{-(\partial q^+/\partial T)|_{T^+}} + \sqrt{-(\partial q^-/\partial T)|_{T^-}}} \quad (26)$$

$$\gamma^- = \frac{\sqrt{-(\partial q^+/\partial T)|_{T^+}}}{\sqrt{-(\partial q^+/\partial T)|_{T^+}} + \sqrt{-(\partial q^-/\partial T)|_{T^-}}}. \quad (27)$$

Summarizing we can say that a cycle of the working fluid consisting of two isotherms at T^+ and T^- connected by two (infinitely fast) isentropes/adiabats produces maximum power.

4 Example: A system in contact with three heat reservoirs

As an example let us consider a system with three heat reservoirs. The temperatures of these reservoirs are T_{01} , T_{02} , and T_{03} . If they are connected to the working fluid the heat exchange follows a linear transport law:

$$q_i(T_{0i}, T) = \kappa_i(T_{0i} - T). \quad (28)$$

We choose the heat conductances κ_i to be equal and without loss of generality we set $\kappa_1 = \kappa_2 = \kappa_3 = 1$ by an appropriate choice of units. For this case of linear heat transport, $q^+(\mathbf{T}_0, T)$ and $q^-(\mathbf{T}_0, T)$ are piecewise linear, whereas $\sigma^+(\mathbf{T}_0, T)$ and $\sigma^-(\mathbf{T}_0, T)$ consist of pieces of rectangular hyperbolae.

This system is one of the simplest possible to discuss the phenomenon of unused reservoirs. In order to do so we fix the temperatures of the hottest and coldest reservoir: $T_{01} = 1$ and $T_{03} = 4$. We then vary the temperature of the intermediate reservoir T_{02} between T_{01} and T_{03} in steps of 0.05 and study how the behavior of the system changes.

Following the above developed theory, the optimal cycle of the working fluid is a Carnot cycle with two isotherms and two isentropes. Thus we determine the two base points for each temperature T_{02} . From those the corresponding heat flows lead to the maximal power and the efficiency at maximal power which all depend on T_{02} .

In figure 6a the indicator function $ind(T_{02})$ shows how the intermediate heat reservoir is used: For low temperatures it is in contact with the working fluid at the same time as reservoir 1, here indicated by $ind = 1$, for high temperatures it is in contact at the same time as reservoir 3 and thus $ind = 3$. In between the reservoir is not used at all: $ind = 0$. One clearly sees the intermediate region where reservoir 2 remains unused.

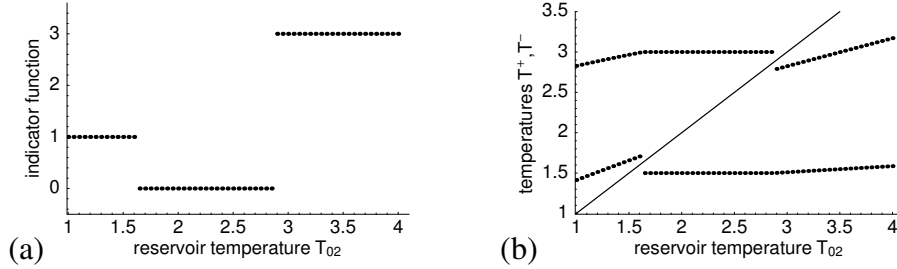


Figure 6: (a) The indicator function $ind(T_{02})$. (b) the temperatures T^+ and T^- as functions of T_{02} . The solid line illustrates T_{02} .

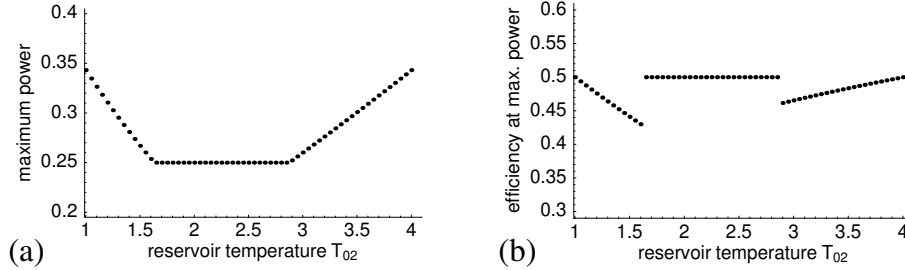


Figure 7: (a) The maximal power output as a function of T_{02} . (b) The corresponding efficiency at maximum power.

In figure 6b the temperatures T^+ and T^- are shown as functions of T_{02} . One sees that with increasing T_{02} both base values increase until reservoir 2 is switched off. In the intermediate regime they remain constant and finally they increase again when reservoir 2 is used again. Note that the base temperatures show discontinuities at the switching temperatures: T^- jumps when reservoir 2 is separated from it, T^+ jumps when reservoir 2 is connected to it.

Figure 7a shows the resulting maximal power output as a function of T_{02} . With increasing T_{02} the power decreases until reservoir 2 is switched off, then it remains constant, and after reservoir 2 is switched on again – but now to the the high temperature branch – the power increases again. In figure 7b the corresponding efficiency at maximum power is shown. In the intermediate regime it attains its maximum value which coincides with the efficiency at the two boundary points $T_{02} = T_{01}$ and $T_{02} = T_{03}$.

Finally we mention that the above discussed behavior can be understood in terms of a Curzon-Ahlborn engine: As in the intermediate regime the system uses only two heat reservoirs the efficiency at maximum power should be that of the Curzon-Ahlborn engine

$$\eta_{CA} = 1 - \sqrt{\frac{T_{01}}{T_{03}}} = 1 - \sqrt{\frac{1}{4}} = 0.5, \quad (29)$$

which it is indeed. An analysis presented in the next section shows that also the T_{02} dependence of the power and the temperatures T^+ and T^- can be analytically determined.

5 Curzon-Ahlborn equivalent engines

In this section the analytical dependence of the temperatures as well as the power production are based on the power optimization of particular Curzon-Ahlborn engines. Let us assume that a Curzon-Ahlborn engine operates between two heat reservoirs at T_H and T_L , to which it is coupled through heat conductances κ_H and κ_L , respectively. For this engine the temperatures at maximum power are

$$T_{CA}^+(T_H, T_L) = \frac{\sqrt{\kappa_H}\sqrt{T_H} + \sqrt{\kappa_L}\sqrt{T_L}}{\sqrt{\kappa_H} + \sqrt{\kappa_L}} \sqrt{T_H} \quad (30)$$

$$T_{CA}^-(T_H, T_L) = \frac{\sqrt{\kappa_H}\sqrt{T_H} + \sqrt{\kappa_L}\sqrt{T_L}}{\sqrt{\kappa_H} + \sqrt{\kappa_L}} \sqrt{T_L}. \quad (31)$$

Note that these temperatures do depend on the heat conductances κ_H and κ_L . The maximum power also depends on the conductances

$$P_{CA, \max}(\kappa_H, \kappa_L, T_H, T_L) = \frac{\kappa_H \kappa_L}{(\sqrt{\kappa_H} + \sqrt{\kappa_L})^2} (\sqrt{T_H} - \sqrt{T_L})^2, \quad (32)$$

while the efficiency at maximum power is independent of the conductances

$$\eta_{CA}(T_H, T_L) = 1 - \sqrt{\frac{T_L}{T_H}}. \quad (33)$$

In figures 8 the lines represent the analytically obtained dependences for three different choices of Curzon-Ahlborn engines: The solid line gives the results for the choice (I) $T_H = T_{03}$ and $T_L = T_{01}$ and $\kappa_H = \kappa_L = 1$. The long dashed line corresponds to choice (II) $T_H = (T_{02} + T_{03})/2$, $T_L = T_{01}$, $\kappa_H = 2$ and $\kappa_L = 1$, i.e. the two reservoirs 2 and 3 have been united into one reservoir. Finally (choice (III)) the short dashed line has $T_H = T_{03}$, $T_L = (T_{01} + T_{02})/2$, $\kappa_H = 1$ and $\kappa_L = 2$, which means that reservoirs 1 and 2 have been combined.

It is seen that the optimal solution corresponds to Curzon-Ahlborn engines with corresponding averages of reservoirs. Note that equating $P_{CA, \max}$ from equation (32) for choice (I) and (III) results in an equation for the lower switching temperature $T_{02}^{(III-I)}$. One finds $T_{02}^{(III-I)} = c_1 \sqrt{T_{01}} + c_2 \sqrt{T_{01} T_{03}} + c_3 \sqrt{T_{03}}$ with coefficients c_1 , c_2 , and c_3 . Likewise $T_{02}^{(I-II)}$ can be determined.

Conclusion

This study considered power producing thermo-mechanical systems exchanging heat with several (more than two) heat reservoirs via irreversible heat transfer processes. The systems were optimised for maximum power output at a

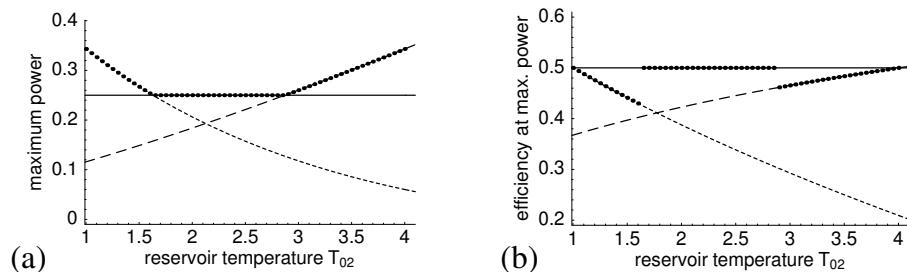


Figure 8: (a) The maximal power output is shown for a three-reservoir system. Dots indicate the optimal solution. The curves are the maximum power output of Curzon-Ahlborn engines with particular choices of reservoirs. Solid: only the extreme reservoirs T_{02} and T_{03} are used. Short dashed: the low-temperature reservoir is the average of T_{01} and T_{02} . Long dashed: the high-temperature reservoir is the average of T_{02} and T_{03} . (b) The efficiency at maximal power output is shown for a three-reservoir system.

given increase of entropy and internal energy of the working fluid for the case of stationary temperatures of the heat reservoirs. We found that independent of the number of reservoirs the temperature of the working fluid should attain no more than two different values. These base values are time independent and are attained for a certain fraction of the overall time available for the process. In particular this is the case for cyclic processes. Here the optimal cycle corresponds to a Carnot cycle of two isotherms and two isentropes/adiabats.

A surprising but inevitable consequence of this process structure is that there may exist heat reservoirs which should never connect to the working fluid. These “unused” reservoirs provide heat at temperatures which lie between the temperatures of the isotherms. Thus it is more advantageous to ignore the heat available from them than to operate at different temperatures.

References

- [1] Morton H. Rubin. Optimal configuration of a class of irreversible heat engines. I. *Phys. Rev. A*, 19(3):1272–1276, 1979.
- [2] M. J. Ondrechen, M. H. Rubin, and Y. B. Band. The generalized Carnot cycle - a working fluid operation in finite-time between finite heat sources and sinks. *J. Chem. Phys.*, 78:4721–4727, 1983.
- [3] K. H. Hoffmann, J. M. Burzler, and S. Schubert. Endoreversible thermodynamics. *J. Non-Equilib. Thermodyn.*, 22(4):311–355, 1997.
- [4] Adrian Bejan. Entropy generation minimization: The new thermodynamics of finite-size devices and finite-time processes. *J. Appl. Phys.*, 79(3):1191–1218, 1996.

- [5] M. J. Ondrechen, B. Andresen, M. Mozurkewich, and R. S. Berry. Maximum work from a finite reservoir by sequential Carnot cycles. *Am. J. Phys.*, 49(7):681–685, 1981.
- [6] Morton H. Rubin and Bjarne Andresen. Optimal staging of endoreversible heat engines. *J. Appl. Phys.*, 53(1):1–7, 1982.
- [7] Jincan Chen and Zijun Yan. Optimal performance of an endoreversible-combined refrigeration cycle. *J. Appl. Phys.*, 63(10):4795–4798, 1988.
- [8] Chih Wu. Power performance of a cascade endoreversible cycle. *Energy Conversion and Management*, 30(3):261–266, 1990.
- [9] S. Jeong and J. L. Jr Smith. Optimum temperature staging of cryogenic refrigeration system. *Cryogenics*, 34(11):929–933, 1994.
- [10] G. De Mey and Alexis De Vos. On the optimum efficiency of endoreversible thermodynamic processes. *J. Phys. D: Appl. Phys.*, 27(4):736–739, 1994.
- [11] J. Chen and C. Wu. Performance of a cascade endo-reversible heat-pump system. *J. Inst. Energy*, 68(476):137–141, 1995.
- [12] Bahri Sahin and Ali Kodali. Steady-state thermodynamic analysis of a combined Carnot cycle with internal irreversibility. *Energy*, 20(12):1285–1289, 1995.
- [13] O. M. Ibrahim and S. A. Klein. High-power multistage rankine cycles. *J. Energy Resources Technology*, 117:192–196, 1995.
- [14] Adrian Bejan. Theory of heat transfer-irreversible power plants - II. the optimal allocation of heat exchange equipment. *Int. J. Heat Mass Transfer*, 38(3):433–444, 1995.
- [15] A. M. Tsirlin. Conditions for optimality of the solution of averaged problems of mathematical programming. *Dokl. Akad. Nauk SSSR*, 323(1):43–47, 1992. in Russian.
- [16] A. M. Tsirlin. *Methods of Averaged Optimization and their Applications*. Nauka-Fizmatlit, 1997. in Russian.
- [17] L. I. Rozonoer and Anatolii M. Tsirlin. Optimal control of thermodynamic processes I. *Automat. Remote Control*, 44(1):55–62, 1983. Translated from *Avtomatika i Telemekhanika*.
- [18] L. I. Rozonoer and Anatolii M. Tsirlin. Optimal control of thermodynamic processes II. *Automat. Remote Control*, 44(1):209–220, 1983. Translated from *Avtomatika i Telemekhanika*.
- [19] L. I. Rozonoer and Anatolii M. Tsirlin. Optimal control of thermodynamic processes III. *Automat. Remote Control*, 44(1):314–326, 1983. Translated from *Avtomatika i Telemekhanika*.

- [20] R. S. Berry, V. A. Kazakov, S. Sieniutycz, Z. Szwast, and A. M. Tsirlin. *Thermodynamic Optimization of Finite-Time Processes*. John Wiley & Sons, Chichester, 2000.